NANO LETTERS
Letter
Cite This: Nano Lett. 2019, 19, 2478−2488
pubs.acs.org/NanoLett

Cellular Metabolomics by a Universal Redox-Reactive Nanosensors Array: From the Cell Level to Tumor-on-a-Chip Analysis

Vadim Krivitsky,*[,†] Marina Zverzhinetsky,[†] Adva Krivitsky,[‡] Lo-Chang Hsiung,[†] Vladimir Naddaka,[†] Itay Gabriel,[§] Sharon Lefler,[†] Jennifer Conroy,[†] Larisa Burstein,[∥] and Fernando Patolsky*[,†,§]

[†]School of Chemistry, the Raymond and Beverly Sackler Faculty of Exact Sciences, Tel-Aviv University, Tel Aviv 69978, Israel
[‡]Department of Physiology and Pharmacology, Sackler Faculty of Medicine, Tel Aviv University, Tel Aviv 69978, Israel
[§]Department of Materials Science and Engineering, the Iby and Aladar Fleischman Faculty of Engineering, Tel Aviv University, Tel Aviv 69978, Israel
[∥]Wolfson Applied Materials Research Center, Tel Aviv University, Tel Aviv 69978, Israel

Supporting Information

ABSTRACT: Although biosensors based on nanowires-field effect transistor were proved extraordinarily efficient in fundamental applications, screening of charges due to the high-ionic strength of most physiological solutions imposes severe limitations in the design of smart, "real-time" sensors, as the biosample solution has to be previously desalted. This work describes the development of a novel nanowire biosensor that performs extracellular real-time multiplex sensing of small molecular metabolites, the true indicators of the body's chemistry machinery, without any preprocessing of the biosample. Unlike other nanoFET devices that follow direct binding of analytes to their surfaces, our nanodevice acts by sensing the oxidation state of redox-reactive chemical species bound to its surface. The device's surface array is chemically modified with a reversible redox molecular system that is sensitive to H_2O_2 down to 100 nM, coupled with a suite of corresponding oxidase enzymes that convert target metabolites to H_2O_2, enabling the direct prompt analysis of complex biosamples. This modality was successfully demonstrated for the real-time monitoring of cancer cell samples' metabolic activity and evaluating chemotherapeutic treatment options for cancer. This distinctive system displays ultrasensitive, selective, noninvasive, multiplex, real-time, label-free, and low-cost sensing of small molecular metabolites in ultrasmall volumes of complex biosamples, in the single-microliter scale, placing our technology at the forefront of this cutting-edge field.

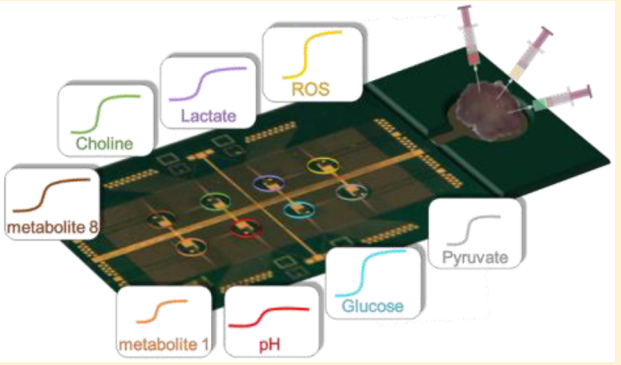

KEYWORDS: *nanowires, field effect transistor, redox, lab-on-a-chip, metabolomics*

Nanowires-based field effect transistor (NW-FET) sensors are a yet untapped means of applying nanobiotechnology for the detection of biological and chemical species. These devices have been proved extraordinarily efficient over planar FET devices, by virtue of their one-dimensional nanoscale morphology,[1] which makes their electrical properties extremely sensitive to species adsorbed on their surfaces, down to the detection of single molecules.[2] The abundant use of biological and chemical sensors nowadays holds the potential for these devices to become a key player to improve our daily lives in a variety of areas such as medical diagnostics,[3,4] drug discovery,[5] scientific research,[6] food and water quality control,[7] environmental monitoring,[8] agriculture,[9] homeland security,[10,11] and more.

NW-FET sensor devices function by sensing the charge of a surface-bound molecule; however, given the high ionic strength of most physiological biosamples, detection of a specific binding event is severely screened (i.e., the Debye screening).[4] For typical biosample solutions (i.e., blood, serum, and urine), with a Debye screening length of approximately 0.7−2.2 nm, the surface potential will be completely hampered at a distance of a few nanometers.[12] Hence, although NW-FET sensor devices offer rapid and prompt analysis of minute amounts of macromolecules with extremely high sensitivity and selectivity, the need of desalting the physiological biosamples prior to their use imposes severe limitations in the design of smart, real-time sensors. Research efforts to overcome this fundamental limitation have been recently reported, demonstrating the successful detection of biomolecules from whole blood[3,4,13] based on approaches that isolate the detector from the complex environment, using large

Received: January 6, 2019
Revised: March 6, 2019
Published: March 18, 2019

DOI: 10.1021/acs.nanolett.9b00052
Nano Lett. 2019, 19, 2478−2488

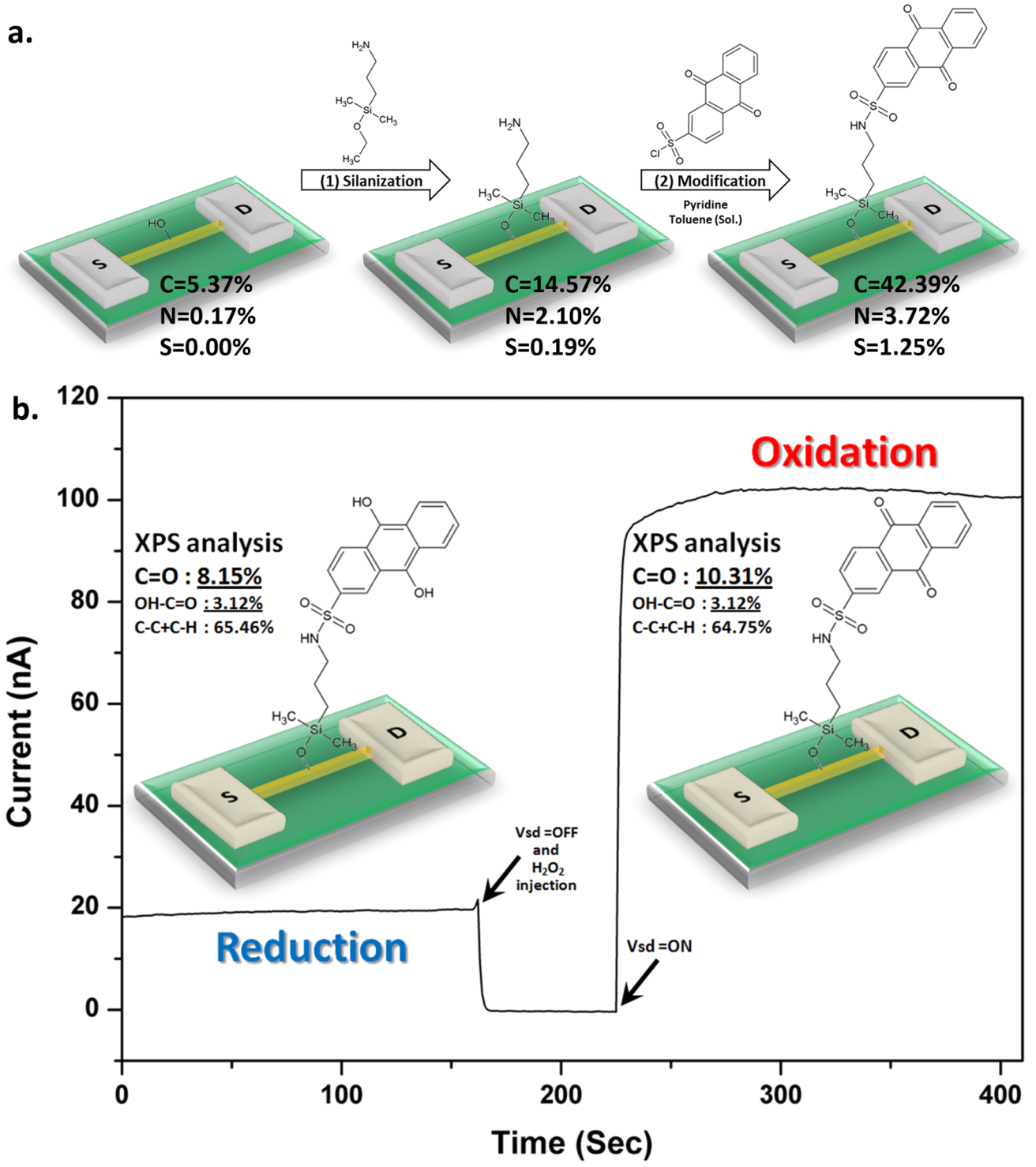

Figure 1. Surface modification and XPS analysis of the redox-reactive SiNW FET. (a) The stages of the surface modification: (1) Silanization of the SiNW activated surface with amine groups; (2) formation of a sulfonamide bond that connects between the 9,10-anthraquinone to the modified surface. The atomic compositions by XPS analysis of the modified surface (for carbon (C), nitrogen (N), and sulfur (S)), following each step of the modification. (b) Reduction of the modified SiNW FET surface by 1% v/v DEHA, followed by oxidation in 1 mM H_2O_2. XPS analysis demonstrates the changes in the concentration of the C═O bond population due to oxidation and reduction processes. The sensing was performed in pH 7.4 in 150 mM phosphate-buffered saline. Before injecting a new sample (800 μL sample, rate = 100 μL/second), the devices were switched off (V_{sd} = 0 V). During the measurement, the source-drain voltage (V_{sd}) was 0.3 V, and the gate voltage (V_g) was 0 V. See Supporting Information Section 7 for detailed XPS spectra.

antibodies as capture agents. This concept mainly bypasses, rather than overcoming, this challenging problem.

Metabolomics refers to the scientific study of the chemical processes of small molecule metabolites including amino acids, peptides, lipids, sugars, oligonucleotides, steroids, alkaloids, organic acids, amines, ketones, and aldehydes and, in some cases, drugs or xenobiotics.[14] Metabolites are the indicators of the body's biochemistry, and as such, the forecast of altered

DOI: 10.1021/acs.nanolett.9b00052
Nano Lett. 2019, 19, 2478−2488

metabolites in a disease can be considered a mirror to the abnormal processes occurring within the body.[15] Whereas in proteomics and genomics only some alterations are directly contributing to the malignant phenotype of a disease, metabolomics may represent the best estimation of the pathogenesis.[16] Therefore, the detection of small metabolite molecular markers is highly important from a clinical point of view, in making inferences regarding pathology. Moreover, the choice of using metabolites as potential biomarkers reflecting an anomaly dismisses the use of bulky antibodies as capture agents and benefits with the detection under high ionic strength biosample solutions without any pretreatment. Given the staggering complexity of cellular processes, the reversible redox-reactive modified sensor is designed to detect non-invasively the extracellular environment, where the accumulation or depletion of metabolites occurs.[17] Traditionally, monitoring of cell signaling-related metabolites (such as reactive oxygen species, ROS), which has significant importance to cellular functions, differentiation, and proliferation, is mainly performed by extracellular sensing methods.[18]

In this work, we report on the development of a novel redox-reactive nanosensor configuration in which silicon NW-FET devices perform extracellular real-time multiplex sensing of small molecular metabolites, without any preprocessing of the biosample. Our approach enables detection directly from complex biosample solutions, with the detected target molecules confined "under the radar", within the ∼0.7 nm Debye screening length. This important achievement was possible due to chemically modifying the nanowires with a reversible redox-active molecular system sensitive to H_2O_2; H_2O_2 being an oxidative species[19] that can selectively react with the redox-reactive reversible system bearing hydroquinone functional groups.[20] Redox reactions involve a significant change in the charge distribution of the participating molecules in close vicinity with the sensor surface,[21] which makes them strong candidates as a recognition layer when introduced on NW-FET sensors. This coupling sensitizes the nanowires to a reversible redox process occurring directly on their surfaces. Furthermore, the high ionic strength functions as a noise filter that maintains a stable signal deriving exclusively from the oxidation of the redox moieties on the SiNW FET surface, where all other substances in the environment are completely screened.

The selectivity of our sensor for specific metabolites was achieved by coupling the redox reaction to a suite of corresponding enzymes, nature's best selectors, which convert the target metabolites to H_2O_2,[22,23] prior to their introduction to the respective nanowire sensing array microfluidic channel. Such a reaction, in which metabolites are converted to H_2O_2, is widely used in bioanalysis by applying oxidase enzymes.[24] However, direct immobilization of oxidase enzymes to the nanodevice's surface[25] increases the complexity and reduces the performance of the device as it is dependent on the enzyme's stability,[26] whereas our redox reactive nanosensor can operate properly and maintain its continuous stability for a period of several weeks. Indeed, several electrochemical sensors immobilized with enzymes can perform direct detection of metabolites without preprocessing of the biosample,[27,28] but they have poor multiplexity and stability, and their miniaturization and integration with complementary metal−oxide−semiconductor (CMOS) technology are limited.

Also, a microfluidic setup was used to flow minute solution samples of metabolites that were converted to H_2O_2 and to follow the oxidation kinetics of the redox-sensitive sensor surface. The combination of this system with microfluidics technology enabled to perform rapid, automated, multiplex and real-time metabolite's detection using minimal sample size.[29,30]

Finally, the redox-reactive sensor device response under physiological conditions was successfully applied for estimating the metabolic activity and evaluating chemotherapeutic treatments in different cell-models of cancer, including solid tumors.

Results and Discussion. *Sensing Principle of the Redox-Reactive SiNW FET.* The 9,10-dihydroxyanthracene/9,10-anthraquinone (DHA/AQ) redox reversible system was selected as the sensing moiety on the SiNW FET array due to the rapid oxidation of the reduced form DHA in the presence of metabolic products such as H_2O_2 and ROS via conversion to the oxidized state AQ, Figure 1b. However, AQ in aqueous solution can be reversibly reduced back to DHA in the presence of mild chemical reductants such as *N*,*N*-diethylhydroxylamine (DEHA), or by applying electric potential.[31] Therefore, by covalently binding this redox system to a SiNW FET device's array surface via a short linker, a novel configuration of redox-reactive SiNW FET nanodevices was achieved, Figure 1a. An additional advantage of using immobilized nanosensor bearing redox-reactive moieties is their ability to restrict undesirable side reactions normally occurring in bulk solutions; hydroquinone-based redox systems tend to create quinhydrone as a result of the reaction between hydroquinone and the oxidized form; quinone.[32,33] In order to prevent this reaction, usually hydroquinone-based redox-reactive systems use metallic catalysts that promote further oxidation of the quinhydrone complex to two quinine molecules.[20] In the case of the presented redox-reactive SiNWs, immobilization of the hydroquinone moieties define their positions on the SiNWs surface, further limiting sterically the formation of the quinhydrone complexes.

The different steps of the chemical modification performed on a p-type SiNW FET array surface were analyzed and supported by using X-ray photoelectron spectroscopy (XPS), Figure 1a. First, the SiNWs surface was oxidized using oxygen plasma in order to clean and activate the surface for the following silanization process. Then, the chip was covered with (3-aminopropyl)-dimethyl-ethoxysilane (APDMES) under argon atmosphere, in order to ensure the formation of a monolayer of silane, which is critical for the successful sensing in physiological solutions, due to Debye length limitations.[34] APDMES is, in addition, long-term stable under physiological conditions, compared to other silane-based modifications.[35] XPS analysis demonstrated the successful binding of the amino-silane derivative as indicated by the increased percentage of nitrogen atoms on the SiNW surface, Figure 1a, middle panel. The amino-modified SiNW FET was then introduced to a solution of 9,10-anthraquinone-2-sulfochloride (AQ-SO_2Cl) under argon atmosphere. Dry conditions are important to prevent the decomposition of the sulfochloride group through hydrolysis.[36] The sulfochloride group reacts with the amino groups on the SiNW FET surface to form a covalent highly stable sulfonamide bond[37] that enables the long-term fixation of AQ moieties to the SiNW FET surface. XPS analysis showed the increased concentration of sulfur atoms following AQ-SO_2Cl modification, which indicates the successful binding of the AQ moiety, Figure 1a, right panel.

DOI: 10.1021/acs.nanolett.9b00052
Nano Lett. 2019, 19, 2478−2488

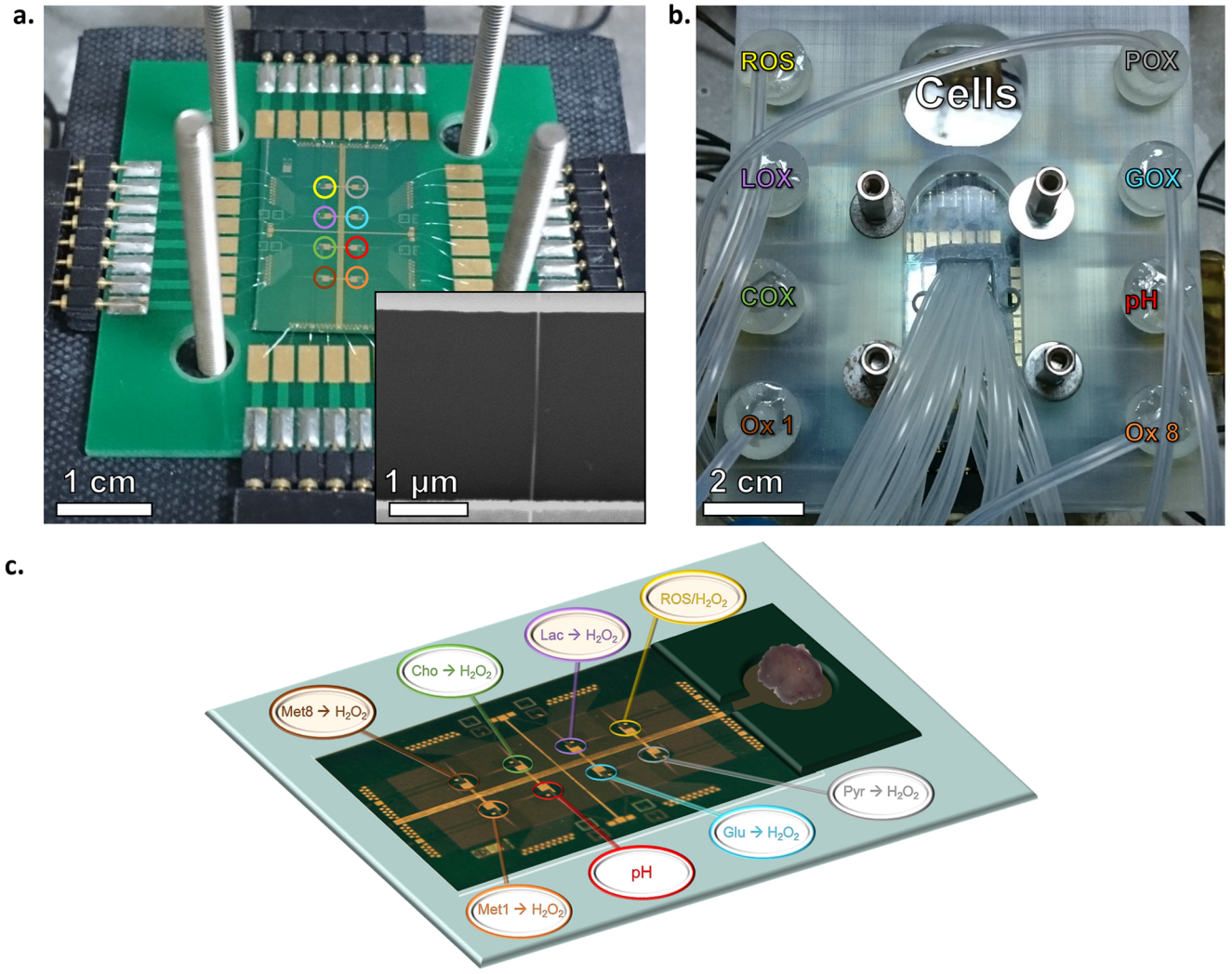

Figure 2. Microfluidic nanowire extracellular biosensor for multimetabolite analysis. (a) Silicon wafer chip, with 600 nm thermal oxide layer, which contains 144 potential redox-reactive SiNW FET devices, sharing a common gate, separated into eight different sensing subregions, which correspond to different metabolites according to colors: yellow, ROS; gray, pyruvate,; lavender, lactate; green, choline; red, pH; brown, metabolite #1; orange, metabolite #8. Inset: scanning electron microscope image of SiNW FET device consisting of 20 nm p-type SiNWs connected to the source and drain electrodes. The SiNWs chip wire-bonded to the PCB holder, which is connected to the electrical "current recording" system. (b) The eight subregions for multiplex analysis separated by using a dedicated eight-channel microfluidic PDMS device. The microfluidic multichannel is placed directly above the SiNWs array, on the chip surface, and attached via the 3D-printed clear resist multiwell sheet and screws. The multiwells sheet includes a compartment for cellular samples with medium (white) and compartment for incubation before metabolic analysis: yellow, without adding nothing for ROS detection; gray, adding pyruvate oxidase (POX); lavender, adding lactate oxidase (LOX); green, adding choline oxidase (COX); red, adding 1% v/v DEHA for pH sensing; brown, adding oxidase 1 (Ox 1) for metabolite 1 sensing; orange, adding oxidase 8 (Ox 8) for metabolite 8 sensing. The extracellular samples were transferred via a pipettor into the incubation compartment. Then, liquids from different wells were introduced to the different sensing subregions through a multimicrochannel for multiplex analysis. (c) Schematic representation of a multiplex real-time monitoring of metabolites platform. The target cells/tumor incubated and monitored via microscope at the cell culture well (cells in white in panel b), then an extracellular sample from the target cells/tumor is transferred to the eight different wells with oxidase enzymes to convert the metabolites to H_2O_2 (Glu, glucose; Lac, lactate; Pyr, pyruvate; Cho, choline, Met1, metabolite #1; Met1, metabolite #8). For pH sensing, 0.1% v/v DEHA is added to the cell tested medium, and for ROS/H_2O_2 analysis, no substance is added to the well. Then the medium flows directly to the sensing area. For detailed fabrication and assembly processes, see Supporting Information Sections 1−4 and 8−10.

When the device was incubated with the reductant DEHA under physiological conditions (150 mM phosphate-buffered saline, pH 7.4), which reduces the AQ moieties on the nanodevice surface to their "reduced state" DHA, a conductivity decrease was observed. Moreover, a decrease in carbonyl (C═O) bonds on the SiNW FET device surface was observed by XPS measurement, Figure 1b. Conversely, when the device was incubated with H_2O_2, still under physiological conditions, the H_2O_2 oxidized the reduced DHA moieties on the nanodevice surface to their "oxidized state" AQ, resulting in increased conductivity of the nanodevice, Figure 1b. The XPS measurement further supported the increase in carbonyl (C═O) bonds on the SiNW FET device surface, which signify a complete successful oxidation−reduction cycle over the redox-reactive SiNW FET device surface. Importantly, XPS analysis showed no change in other types of carbon bonds (C−C + C−H bonds or HO−C═O bonds) due to the reduction and oxidation processes, which means that the change in the

DOI: 10.1021/acs.nanolett.9b00052
Nano Lett. 2019, 19, 2478−2488

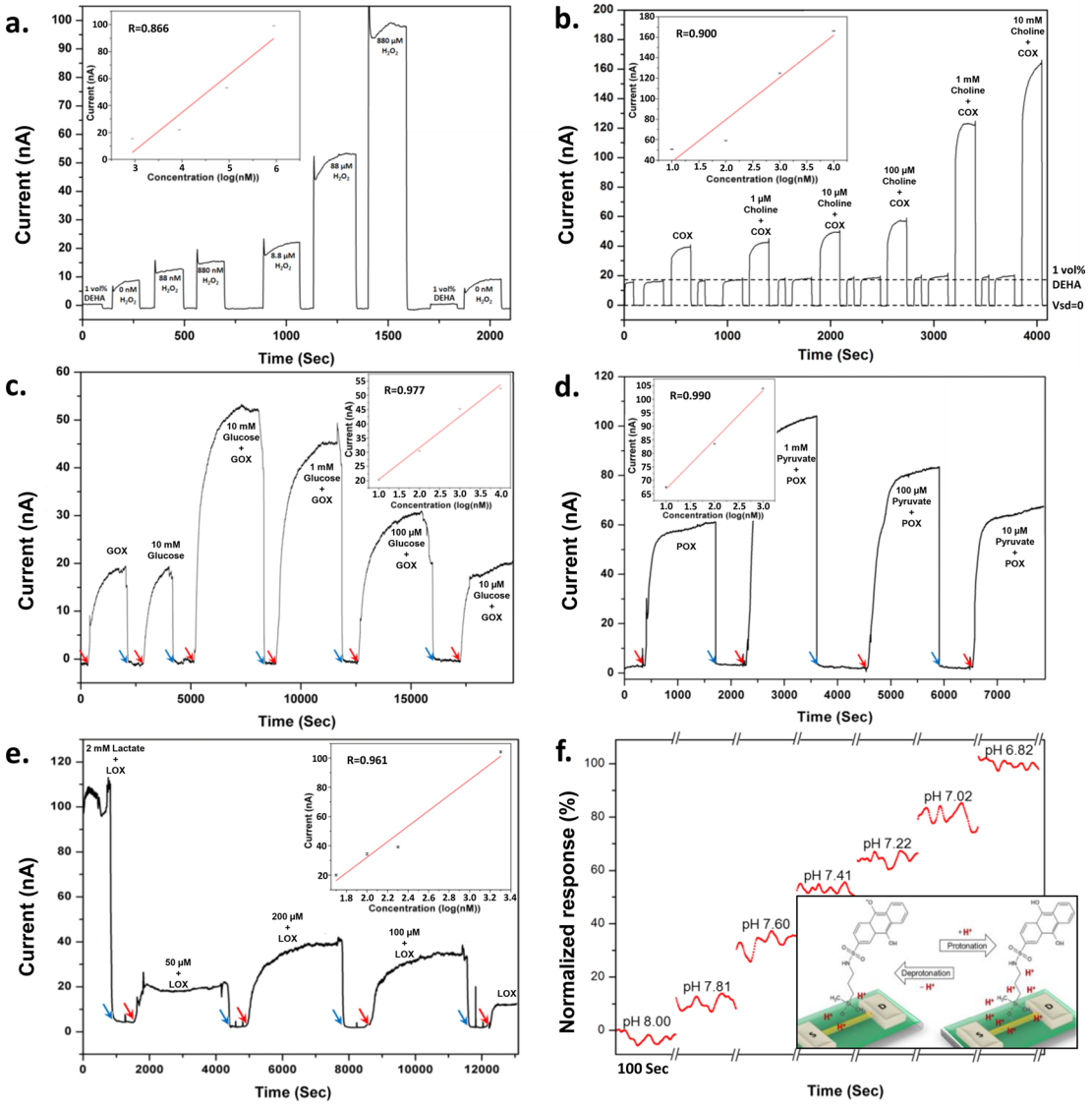

Figure 3. Multimetabolites detection under physiological conditions. A SiNW FET array is modified with AQ-SO_2Cl for sensing of ROS, choline, lactate, glucose, and pyruvate. Before metabolites reach the FET array, small-molecule metabolites are converted to hydrogen peroxide (H_2O_2) by oxidase enzymes. Then, either the ROS or the H_2O_2 oxidizes the DHA that is bound to the NW FET surface to form AQ. A reductant, DEHA (1% v/v), reduces AQ to DHA to restore the device toward another detection cycle. (a-e), Sensing of increasing concentrations of (a) H_2O_2, performed by manual injection and measurement under nonflow conditions, in RPMI cell culture medium supplemented with 10% fetal bovine serum; (b) Choline, performed by manual injection and measurement under nonflow conditions, in PBS; (c) glucose, (d) pyruvate, and (e) lactate, performed by the flow mode in PBS, revealed linear correlation between the obtained current and the log of analyte concentrations. Following each analysis, the device's current was restored to its initial level by the injection of 1% v/v reductant (DEHA reduction process, marked by a blue arrow in panels c–e). In static mode (panels a and b), the devices were switched off during the injection of 1% v/v reductant before the samples exchange, in order to reduce the electrical noise levels as a result of the exchange. In continuous flow mode (panels d and e), each injection of the sample is marked by a red arrow. The calibration curve (panels a–e) was extracted from the current values of each measurement, right before the devices were switched off (panels a and b) or the injection of DEHA (panels c–e). See Supporting Information Sections 15 and 16 for detailed sensing protocols and current values (*Y*-axis) errors estimation. (f) Conversion of the modified FET into a pH sensor was achieved by using a reductant-added solution. After supplementing a culture medium with 0.1% v/v DEHA to reduce the modified FET surface and ROS/H_2O_2 content, surface proton density varied by protonation or deprotonation dominantly changes the measured current (inset f). See Supporting Information Section 11 for the normalized response calculation and the reversibility of the pH measurements.

conductivity has derived solely from alterations in C═O bond population, Figure 1b, and the oxidation–reduction state of the monolayer. As anticipated, the conductivity of the nanodevice depends on the population of reduced (DHA)/oxidized (AQ) states of the reversible redox system moieties on the SiNW FETs surface.

Multimetabolites Detection under Physiological Conditions. Small molecule metabolites secreted by pathological processes have been under intense research as molecular biomarkers for clinical diagnosis.[38] Their detection is of great significance, as it may represent the best estimation of the pathogenesis of a disease and provide the biochemical phenotype for drug treatment.[39,40] Another aspect is that the detection is performed extracellularly, in contrast to other "omics" methods, as the accumulation of metabolites occurs outside the cells. With the release of the Human Metabolome

DOI: 10.1021/acs.nanolett.9b00052
Nano Lett. 2019, 19, 2478–2488

Database, a decade ago,[41] small metabolites screening holds a great potential to become a standard screening method embracing many areas of our lives, from personalized medicine up to recommendations about lifestyle or nutrition.[42] Among the analytical techniques that can be employed for metabolomics applications, nuclear magnetic resonance (NMR) spectroscopy and mass spectrometry (MS) combined with separation techniques are the most common.[43] Although they show intrinsic high sensitivity in detection from complex biofluids, these instruments are expensive, and many of them require considerable skill for their operation, therefore becoming inadequate for mass use and real-world applications.

Hence, our novel redox-reactive nanosensor platform for the detection of small molecular metabolites offers a key set of functions, enclosing unique properties in a single device that ultimately are translated to ultrasensitive, selective, non-invasive, multiplex, real-time, label-free, and low-cost sensing of minute volume metabolites from complex biosamples.

In order to continuously monitor concentrations of extracellular ROS and additional metabolites, a detection system must be designed that ideally does not alter productions of target metabolites or perturb their associated extracellular concentrations.[44] Accordingly, a microfluidic nanowire biosensor, including a cell/tissue culture compartment and a separate sensing compartment, Figure 2, was designed. The former includes wells for the incubation of cell samples, connected to the sensing compartment by microfluidic channels that deliver the extracellular sample, the oxidase enzymes, or the reducing agent (1% V/V DEHA) from their respective wells, Figure 2b. Then, the fluids from the different wells are introduced into the eight separated sensing compartments, through a multi-microchannel system for their multiplex analysis, as previously described.[10] A SiNWs FET array, Figure 2a, inset, the core of the sensing compartment, was modified with AQ-SO_2Cl for sensing of ROS, or H_2O_2, converted from the individual metabolites, Figure 2c. Before metabolites reach the FET array, small-molecule metabolites are converted to H_2O_2 by the corresponding oxidase enzymes and separately delivered through each of the eight microchannels leading to the sensing subcompartments, Figure 2b. Then, ROS, or the resulting H_2O_2, oxidizes the reduced DHA on the corresponding nanoFET device surface to form the oxidized AQ. This oxidation reaction causes an increase in the current that flows through the p-type SiNW FETs, Figure 1b, right panel. In contrast, incubation in the presence of the reductant DEHA reduces the oxidized AQ back to their reduced state DHA. Thus, the surface charge density varies by oxidation, or by reduction, of the quinone-based reversible redox system, leading to changes in the nanoFETs measured current. After each measurement cycle, the reductant DEHA was used to reduce the nanoFET devices surface, Figure 1b, left panel, for subsequent measurement cycles.

Importantly, by the advantage of microfluidics, only a submicroliter-scale volume of the cellular media and the oxidase enzymes were required to convert metabolites to H_2O_2 for the redox-reactive nanowire biosensor's measurements. Thereby, as a result, by directly mixing a microvolume of oxidase enzymes with target metabolites in the sample, a number of advantages were achieved: (1) maximized species of metabolites detected; (2) the sensing reliability was significantly improved; (3) the lifetime of the sensor was considerably prolonged.

Additional advantages of the proposed microfluidic nanowire biosensor include minimizing the detection time and sample consumption, multiplexing, and real-time detection. Furthermore, by employing multichannel sensing architecture, different samples can be analyzed simultaneously, easily achieving multiplex sensing. Moreover, based on the aforementioned sensing mechanism of NW FETs, there is no need to add any harmful chemicals to cells in order to enable an assessment. Therefore, real-time measurements can be performed to observe metabolic changes in extracellular activity over time.

The redox-reactive SiNW FETs array was first calibrated for sensing of H_2O_2, glucose, pyruvate, lactate, choline, and pH, under physiological conditions, such as in serum-containing cell culture medium, Figure 3. The signals obtained for the detection of different concentrations of H_2O_2 concentrations were highly correlated (correlation coefficients $\approx$ 0.9, Figure 3a) and covered the physiological range of extracellular H_2O_2 concentration, 10 nM to 10 μM, with the lowest detection limit in the range of 1 nM.[45] H_2O_2/ROS play a key role in cellular signaling and are normally produced as a byproduct of metabolism. However, increased ROS/H_2O_2 production may lead to "oxidative stress" and signifies the development of various diseases.[18] Importantly, following reduction of the nanodevices surface by the reductant DEHA, the current returns to its original baseline, which demonstrates the reversibility and reusability capabilities of our redox-reactive SiNW FETs, Figure 3a. As a control experiment, a device modified solely with the APDMES amino-silane linker, without further redox-reactive modification, was tested against H_2O_2 solutions, showing no response up to a concentration of ca. 1 mM, which is considerably above the physiological concentrations of H_2O_2, Supplementary Figure S12.

In order to use these settings for the detection of additional molecular metabolites, there is a need to convert the corresponding metabolites to H_2O_2 by a highly specific reaction. Such a reaction to convert metabolites to H_2O_2 is widely used in bioanalysis by applying oxidase enzymes.[24] Importantly, because enzymes are highly efficient catalysts, the required amount of enzymes is minuscule. Choline is an important metabolite in various physiological processes such as neuronal functions and muscles control.[46] Furthermore, choline has also a role in abnormal cancerous metabolism.[47] In order to perform sensing of choline by the redox-reactive SiNW FET devices, the choline metabolite was specifically converted to H_2O_2 by shortly incubating it with the choline oxidase enzyme (COX). The signals that were measured correlated well with the concentration of choline tested (correlation coefficients = 0.90, Figure 3b) and covered the extracellular choline physiological concentration range (around 7−20 μM).[46] Importantly, after every reduction cycle of the SiNW's surface by DEHA, the current returns to the original baseline, as was previously shown, which indicates the regeneration capability of our devices.

In vitro detection of metabolites is routinely used for monitoring and determining the prognosis of metabolic disorders such as diabetes and cancer.[48] For instance, diabetes is diagnosed by evaluating the concentration of glucose in the plasma and is characterized by a glucose concentration of $\geq$7.0 mM.[49] Also, a routine procedure in radiation oncology is following the uptake of the radiolabeled glucose analog fluorodeoxyglucose (^{18}F-FDG).[50] As glucose consumption is elevated in cancer cells, this compound accumulates in tumors

DOI: 10.1021/acs.nanolett.9b00052
Nano Lett. 2019, 19, 2478−2488

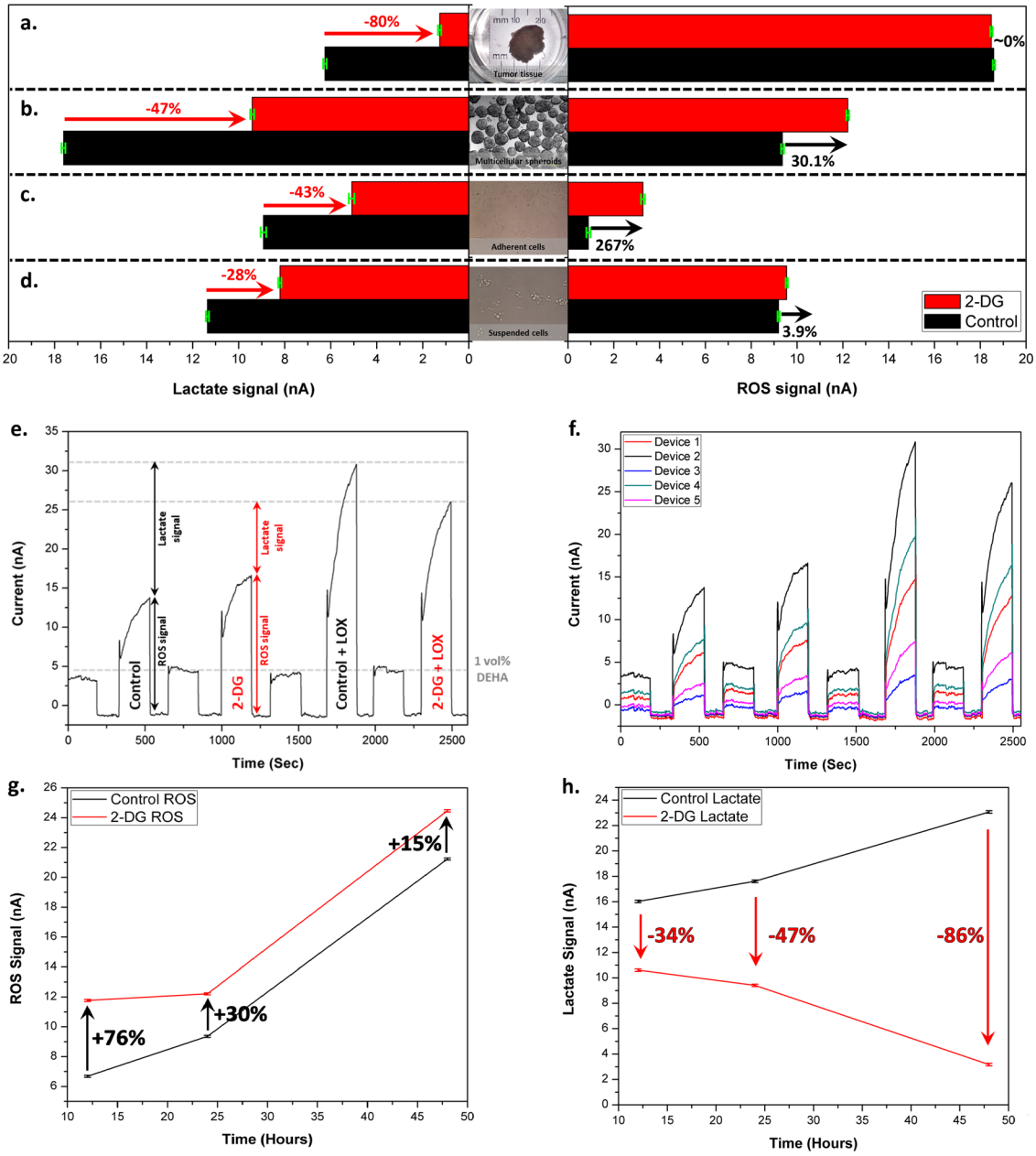

Figure 4. Measuring the effect of 2-DG on different cancer models. Lactate and ROS were detected directly in the cancer cell samples. (a) Tumor tissue (YDFR.SB3 melanoma, 98 mg tumor size), (b) multicellular spheroids (MCF7, 1.65 × 10^6 cell/mL), (c) adherent cells (A549, 1.1 × 10^6 cells/mL), and (d) suspended cells (TK-1, 0.93 × 10^6 cells/mL). In panels a–d, the signal obtained after 24 h from 2-DG treatment, without preprocessing steps, and each measurement was performed by a different device. Panel e demonstrates representative row data obtained by redox-reactive SiNW FETs, as measured during 2-DG effect on a multicellular spheroid cancer cells sample. Before injecting a new sample (800 μL sample, rate = 100 μL/second), the devices were turned off (V_{sd} = 0 V). During each measurement, the source-drain voltage (V_{sd}) was 0.3 V, and the gate voltage (V_g) was 0 V. The lactate signal was constructed from current values of each measurement, right before switching off the device (V_{sd} = 0 V). The signal was calculated by subtracting the value of the current after the addition of oxidase from the value of the current before its addition. The gray line marks the baseline obtained by the addition of reductant (1 vol % DEHA in medium). The lactate and ROS signals for the control are marked in black. The lactate and ROS signals for the 2-DG marked are in red. Panel f demonstrates the same measurement in panel e that was performed by five different redox-reactive SiNW FET devices of the same array to give a similar trend. Panels g and h demonstrate the ROS and lactate signal versus time, after treating the multicellular spheroids with 2-DG. See Supporting Information Sections 15 and 16 for detailed cells culturing protocols and errors estimation in the graphs.

and can be visually tracked by positron emission tomography (PET) scans, thus facilitating diagnosis, staging, and treatment managing.[51,52] Thus, we hypothesize that by monitoring the local levels of glucose, lactate, and the intermediate metabolite that ferments to produce lactate, pyruvate, we could detect metabolic transformations and track cancer on its first stages. In accordance, our sensor was calibrated to detect these metabolites using the enzymes glucose oxidase (GOX), lactate oxidase (LOX), and pyruvate oxidase (POX), which convert them to H_2O_2. Importantly, when GOX and glucose were introduced separately to the devices, no difference between the two signals was observed, but when both were introduced

DOI: 10.1021/acs.nanolett.9b00052
Nano Lett. 2019, 19, 2478−2488

together to the redox-reactive sensor, a concentration-dependent signal for glucose was detected, Figure 3c. For all the three metabolites (glucose, lactate, and pyruvate) sensing, a concentration-dependent signal was obtained as in previous cases (correlation coefficients were 0.977, 0.990, and 0.961 for glucose, pyruvate, and lactate, respectively), Figure 3c–e. Importantly, the sensitivity of the nanodevice covered the physiological concentration range of extracellular glucose,[53] lactate,[54] and pyruvate.[55] Significantly, following every reduction of the nanodevice by the reductant DEHA, the current returns to the original baseline, as was previously shown. For the multiplexed sensing of small molecular metabolites, pH monitoring is vital in a vast variety of fields, starting from basic chemical studies, through chemical and biochemical analysis to medicine and industry. Consequently, great motivation exists for developing innovative, robust, fast, compact, biocompatible, selective, and extremely sensitive pH sensors for extremely small fluid volumes, in the microliter range. Importantly, on the one hand, SiNWs FET-based sensors are highly sensitive to pH, while, on the other hand, living cells excrete acidic metabolites to the extracellular medium during their metabolic activity, which leads eventually to acidification of the medium.[56] Therefore, in order to perform analytical monitoring of small molecular metabolites for relatively long times, it is critical to differentiate between the two separate influences on the conductivity of the nanodevice, the one caused from the pH changes and the other influenced by ROS/H_2O_2 production. Thus, our ROS-sensitive chemically-modified nanoFET array device was converted into a selective pH sensor, by the addition of a reducing agent, Figure 3f inset. For pH sensing, 0.1% v/v of the reductant DEHA was added to the ROS-containing cellular sensing medium to reduce the oxidized AQ monolayer on the FET surface to the reduced DHA state, Figure 1b. Therefore, the addition of physiological concentrations of H_2O_2 in a reductant-added medium[57,58] did not alter the measured signal (Supplementary Figure S10), while alterations of the surface proton density, varied only by protonation or deprotonation events, dominantly changed the acquired signal. Markedly, based on our observations, adding 0.1% v/v DEHA to culture medium did not cause a significant change in the pH. Moreover, a pH-dependent sensing response in the reductant-added medium was observed, Figure 3f. Specifically, the pH sensing sensitivity was below 0.2 pH units per 10% of the device's response, and the detection capability covered the physiological pH range.[59] Furthermore, sensing of H_2O_2 in reductant-free medium and reductant-added medium were compared in Supplementary Figure S10. Therefore, by using a reductant-supplemented solution, pH sensing specificity of the DHA-modified NW FET was demonstrated. Thus, the universal chemistry in which H_2O_2 is formed by the activity of an oxidase enzyme allows us to sense various metabolites simultaneously. Importantly, this sensing method is not limited to those metabolites having corresponding oxidase enzymes and can be further applied for additional metabolites by using a cascade of enzymatic reactions that ends with an oxidase enzyme and the subsequent H_2O_2 production.

Cancer Metabolomics on a Chip. A growing body of evidence suggests that cancer can be considered a metabolic disease.[60] Cancer metabolism is traditionally associated with high glucose consumption and lactate secretion;[61] nonetheless, recent metabolomics studies revealed a positive correlation between various metabolites to the disease stage. In addition, many metabolites demonstrated differential distribution between the tumor and its adjacent healthy tissue.[62] Furthermore, attempts were made to target cellular metabolism as an anticancer therapeutic strategy, using the glucose analog 2-deoxy-D-glucose (2-DG), which is known to inhibit glycolysis.[63,64] Hence, a real-time method for metabolites sensing is an unmet medical need, both in cancer diagnostics and treatment. The sensitivity of the sensor is a matter of high importance, as typically only a small volume of tissues is obtained through a biopsy,[65] while in other cases tumor tissue is unavailable for biopsy. Due to these concerns, a noninvasive multimetabolite test on a minimal number of cells is highly desirable; for instance, a simple blood test that could assess the development of certain cancers. In today's clinics, circulating tumor cells (CTCs), which are diffusional cancer cells deriving from a primary tumor carried around in the circulation system, may represent a valid and accessible source of tumor tissue in the form of "liquid biopsy"; however, the rarity of viable CTC in the peripheral blood makes their clinical use limited.[66]

Hence, our redox-reactive sensor configuration was calibrated for metabolite screening of a minimal number of cancer cells, ca. 10^4–10^6 cells/mL. As aerobic glycolysis produces lactate, monitoring the secreted lactate of drug-treated versus untreated cancer cells may provide an estimation of the efficacy of the drug treatment (Figure 4). In order to convert lactate to H_2O_2, the samples were incubated with LOX enzyme as described before. In addition, the relative stress that was experienced by the cells in response to the drug treatment was evaluated. The amount of stress is correlative to the amount of ROS that was secreted by the cells.[67] ROS can react specifically with the "reduced" DHA monolayer on the nanodevices surface, without the addition of oxidase enzymes.

Hence, we further examined the lactate and ROS metabolism of adherent (Figure 4c) and suspended (Figure 4d) cancer cells in response to 2-DG treatment. Human A549 lung adenocarcinoma adherent cells were seeded at a density of 15,000 cells/cm^2. Murine TK-1 T-cell lymphoma cells were suspended at a density of 0.93×10^6 cells/mL. Both cell lines were treated with 10 mM 2-DG for 24 h, then the medium was collected and transferred to the nanoFET device compartment for the subsequent measurement of lactate and ROS secretion. As expected, a significant decrease in lactate secretion was observed in the samples treated with 2-DG, probably due to the glycolysis inhibition effect of the drug. In addition, A549 cells experienced stress in response to the 2-DG treatment, as indicated by 267% ROS secretion compared with untreated cells. Importantly, the treatment did not affect the cell's viability, as both cell lines were manually counted and analyzed for cellular death following the treatment, and showed no difference between the treated cells and untreated control cells. These results demonstrate the potential of our nanoFET sensor for the real-time metabolic evaluation of anticancer treatment on patients at different developmental stages of the disease.

As cancer is truly a complex disease, a high level of heterogeneity exists at the single cell level between the primary tumor and the metastatic sites,[68] which makes the clinical stage of the disease difficult to assess. Traditional monolayer cultures, or currently used preclinical models, may not assess critical features of the disease or mimic its cellular composition, and so, fail to predict the response to therapy. Spheroids are sphere-shaped cell colonies formed by self-assembly that serve as good 3D tumor models, as they mimic avascular tumors and

DOI: 10.1021/acs.nanolett.9b00052
Nano Lett. 2019, 19, 2478–2488

micrometastases,[69] and are also compatible with microfluidics and miniaturized devices.[70]

As our redox-reactive nanosensors platform monitors metabolites secreted to the extracellular solution, and does not require the direct presence of cells placed on the sensing chip compartment, it is compatible with any cell model, not handicapped to any certain cell configuration. All cellular populations including the original and subgroups of the primary cancerous cells can be sampled and monitored with no restriction. Taking a minimal section of tumor samples from patients and analyzing their metabolism or their response to various drugs can be a guiding tool to better fit the best-personalized treatment for a certain patient.[71] As such, glucose flux technology is ideally suited for understanding cancer and patient response to drug therapy.[22] Taken this distinctive feature, we evaluated the effect of 2-DG on cancer's metabolism of multicellular cancer spheroids (Figure 4b,g,h, Supporting Information Section 12.3 and Figure S11), using the redox-reactive nanosensors platform. Spheroids formed from the human breast epithelial adenocarcinoma cells MCF7 were treated with 10 mM 2-DG for 24 h. The medium was then collected and transferred to the nanoFET device compartment for lactate and ROS sensing. Forty-seven percent reduction in lactate secretion was observed in response to the treatment, simultaneously to an increase of 30% in ROS secretion, compared with untreated control cells. The raw data obtained by our redox-reactive SiNW FETs during the sensing performed on the multicellular spheroids is demonstrated in Figure 4e. The data analysis method is representative of the bar-graphs depicted in Figure 4a−d. ROS signal was the row maximum value of the current as was measured by the device. Lactate signal was calculated by subtracting the "ROS signal" from the maximum value of current that was measured after incubating the medium derived from the spheroids with LOX, the enzyme that converts lactate to H_2O_2. In between samples, the nanoFET devices were switched-off, to avoid the background noise accompanying fluid-exchange via the microfluidics. Figure 4f demonstrates the signals obtained by the five different nanoFET devices that construct the sensing compartment of the chip, during the multicellular spheroids sensing experiment. All five nanoFET devices showed a similar trend in response to the different treatment groups, which varied only by the signal amplitude, demonstrating the high reproducibility of our sensing method. Time-course sensing of ROS and lactate following treatment of the MCF7 spheroids is presented in Figure 4g,h and shows that ROS secretion was 76% higher in the 2-DG treated spheroids compared with untreated cells following 10 h from the treatment, with time the gap between the groups reduced to 15%. The difference in lactate signal between the 2-DG treated spheroids and control, however, increased with time, from −34% up to −86% at 48 h following treatment, demonstrating overtime simultaneous monitoring of metabolites. Finally, we evaluated the performance of our nanoFET devices on a section of solid tumor (Figure 4a, Supporting Information Section 12.4). YDFR.SB3 melanoma cells were subcutaneously injected to nude mice. Forty-five days later, when the tumors reached the size of ∼2.0 cm × 1.5 cm, mice were sacrificed, and the tumors were collected and sectioned. Tumor sections were treated with 10 mM 2-DG for 24 h, then the medium was collected for sensing as previously described. As shown, the redox-reactive platform effectively managed to estimate the anticancer effect of the 2-DG drug, as a decrease of 80% in lactate signal was observed compared with untreated tumor sections. Hence, all four cancer models validated the effectiveness of our nanoFET devices in sensing the response to anticancer treatment. Importantly, the different metabolic patterns of treated and untreated multicellular cancer spheroids could be easily realized after less than 12 h from the onset of the 2-DG treatment. This important feature enables to potentially formulate a personalized treatment strategy for the patient in a short period of time. Moreover, the effect of the drug could be monitored and evaluated over time, and this means screening the most effective drugs and finding the Achilles' heel of cancer resistance to chemotherapy.[72]

Conclusions. Our redox-reactive SiNW FETs platform represents the first nanosensors approach allowing the simultaneous detection of multiple metabolites in physiological fluids. Its ability to perform efficient metabolites detection under physiological conditions, without preprocessing of the samples, is not limited to the metabolites exemplified herein (H_2O_2, choline, glucose, and pyruvate); and it can be further broadened to answer the needs of any metabolite's detection having a corresponding oxidase enzyme (or a peroxide forming enzyme). The platform is fully compatible with CMOS technology, as well as with microfluidics technology similar to other SiNW FET-based sensors.

Our redox-reactive sensor devices' major advantage is their ability to perform sensitive electrical sensing measurements under high ionic strength solutions, such as physiological fluids, where ions in the solution fully and effectively screen all charges in the close environment of the nanowire FET, beyond the <1 nm screening length, except for the charges deriving exclusively from the oxidation/reduction of the surface-confined redox moieties on the intimate vicinity of the SiNW FETs surface. Moreover, its coupling with enzymatic reactions has a significant advantage of selectivity over nonenzymatic methods, as enzymes are designed by natural selection to specifically and selectively fit their biochemical role.[73]

Our redox-reactive SiNW FET sensors have not reached yet their full potential, and can be further exploited as a tool for *in vivo* continuous monitoring of metabolites in patients with other metabolic disorders, such as diabetes.[74] Reversible redox systems like DHA/AQ can alternatively be directly switched on the nanosensors surface by simply applying a voltage stimulus,[75] enabling miniaturization of the nanodevice into implantable dimensions with no need of chemical reducing agents. In addition, the low energy demands of our nanodevice may facilitate their integration within *in vivo* settings.

Finally, our nanodevices were able to perform concentration-dependent sensitive and selective sensing of multiple metabolites in their physiological concentration range (from nanomolar to micromolar concentrations) and were successfully applied for estimating the metabolic activity and evaluating chemotherapeutic treatments for cancer in a lab-on-a-chip setting, applications that have the potential to underscore breakthrough technologies in this field and underpin animals-free, personalized, rapid, and reliable future treatments.[76]

■ ASSOCIATED CONTENT

Supporting Information

The Supporting Information is available free of charge on the ACS Publications website at DOI: 10.1021/acs.nanolett.9b00052.

DOI: 10.1021/acs.nanolett.9b00052
Nano Lett. 2019, 19, 2478−2488

SiNW p-type synthesis, SiNW FET array fabrication, electrical characterization of SiNWs devices, scanning electron microscope analysis, surface modification protocol, mass spectra analysis 9,10-anthraquinone-2-sulfochloride, XPS surface chemistry analysis, fabrication of fluid-delivery system, fabrication of multiwell sheet for multimetabolite analysis, electrical measurements with chemically modified SiNWs FET devices, pH analysis, cancer cells culture and handling, material for metabolic analysis, sensing of H_2O_2 using APDMES-modified SiNW FETs, multimetabolites detection conditions and error analysis (PDF)

AUTHOR INFORMATION

Corresponding Authors

*E-mail: fernando@post.tau.ac.il.
*E-mail: vadimkri@mail.tau.ac.il.

ORCID

Fernando Patolsky: 0000-0002-1382-5357

Notes

The authors declare no competing financial interest.

ACKNOWLEDGMENTS

This work was in part financially supported by the Legacy Fund, Israel Science Foundation (ISF).

REFERENCES

(1) Mulchandani, A.; Myung, N. V. *Curr. Opin. Biotechnol.* **2011**, *22* (4), 502−508.
(2) Patolsky, F.; Zheng, G.; Hayden, O.; Lakadamyali, M.; Zhuang, X.; Lieber, C. M. *Proc. Natl. Acad. Sci. U. S. A.* **2004**, *101* (39), 14017.
(3) Krivitsky, V.; Hsiung, L.-C.; Lichtenstein, A.; Brudnik, B.; Kantaev, R.; Elnathan, R.; Pevzner, A.; Khatchtourints, A.; Patolsky, F. *Nano Lett.* **2012**, *12* (9), 4748−4756.
(4) Krivitsky, V.; Zverzhinetsky, M.; Patolsky, F. *Nano Lett.* **2016**, *16* (10), 6272−6281.
(5) Patolsky, F.; Zheng, G.; Lieber, C. M. Nanowire-based biosensors. *Anal. Chem.* **2006**, *78*, 4260.
(6) Patolsky, F.; Zheng, G.; Lieber, C. M. *Nanomedicine* **2006**, *1*, 51.
(7) Dasgupta, N.; Ranjan, S.; Ramalingam, C. *Environ. Chem. Lett.* **2017**, *15*, 591.
(8) Ghayvat, H.; Mukhopadhyay, S. C.; Gui, X. Sensing Technologies for Intelligent Environments: A Review. In *Intelligent Environmental Sensing*; Springer: 2015; pp 1−31.
(9) Kaur, J.; Pathak, T.; Singh, A.; Kumar, K. Application of Nanotechnology in the Environment Biotechnology. In *Advances in Environmental Biotechnology*; Springer: 2017; pp 155−165.
(10) Lichtenstein, A.; Havivi, E.; Shacham, R.; Hahamy, E.; Leibovich, R.; Pevzner, A.; Krivitsky, V.; Davivi, G.; Presman, I.; Elnathan, R. *Nat. Commun.* **2014**, *5*, 4195.
(11) Engel, Y.; Elnathan, R.; Pevzner, A.; Davidi, G.; Flaxer, E.; Patolsky, F. *Angew. Chem., Int. Ed.* **2010**, *49* (38), 6830−6835.
(12) Stern, E.; Wagner, R.; Sigworth, F. J.; Breaker, R.; Fahmy, T. M.; Reed, M. A. *Nano Lett.* **2007**, *7* (11), 3405−3409.
(13) Stern, E.; Vacic, A.; Rajan, N. K.; Criscione, J. M.; Park, J.; Ilic, B. R.; Mooney, D. J.; Reed, M. A.; Fahmy, T. M. *Nat. Nanotechnol.* **2010**, *5* (2), 138−142.
(14) Tzoulaki, I.; Ebbels, T. M.; Valdes, A.; Elliott, P.; Ioannidis, J. P. *Am. J. Epidemiol.* **2014**, *180* (2), 129−139.
(15) Fiehn, O.; Spranger, J. *Metabolic Profiling: Its Role in Biomarker Discovery and Gene Function Analysis*; Kluwer Academic Publishers: Boston, 2003; pp 199−215.
(16) Nicholson, J. K.; Lindon, J. C.; Holmes, E. *Xenobiotica* **1999**, *29* (11), 1181−1189.
(17) Bittar, E. E. *Metabolic Pumps and Intracellular Homeostasis, Hormones and Cell Function, Intercellular Communication, Cell Motility and Contractility*; JAI Press: 1992.
(18) Thannickal, V. J.; Fanburg, B. L. *American Journal of Physiology - Lung Cellular and Molecular Physiology* **2000**, *279* (6), L1005−L1028.
(19) Gomes, A.; Fernandes, E.; Lima, J. L. F. C. *J. Biochem. Biophys. Methods* **2005**, *65* (2−3), 45−80.
(20) Owsik, I.; Kolarz, B. *J. Mol. Catal. A: Chem.* **2002**, *178* (1−2), 63−71.
(21) Marcus, R. A. *J. Chem. Phys.* **1956**, *24* (5), 966−978.
(22) Munoz-Pinedo, C.; El Mjiyad, N.; Ricci, J. E. *Cell Death Dis.* **2012**, *3*, e248.
(23) Pörtner, R. *Animal Cell Biotechnology: Methods and Protocols*, 2nd ed.; Humana Press: Totowa, NJ, 2007; p xv.
(24) Nakamura, K.; Aizawa, M.; Miyawaki, O. *Electro-enzymology Coenzyme Regeneration*; Springer: Berlin Heidelberg, 2013.
(25) Ansari, S. A.; Husain, Q. *Biotechnol. Adv.* **2012**, *30* (3), 512−523.
(26) Xiao, Y.; Patolsky, F.; Katz, E.; Hainfeld, J. F.; Willner, I. *Science* **2003**, *299* (5614), 1877−1881.
(27) Derfus, G. E.; Abramzon, D.; Tung, M.; Chang, D.; Kiss, R.; Amanullah, A. *Biotechnol. Prog.* **2009**, *26* (1), 284−292.
(28) Wu, M.; Neilson, A.; Swift, A. L.; Moran, R.; Tamagnine, J.; Parslow, D.; Armistead, S.; Lemire, K.; Orrell, J.; Teich, J.; Chomicz, S.; Ferrick, D. A. *Am. J. Physiol-Cell Ph* **2007**, *292* (1), C125−C136.
(29) Patolsky, F.; Zheng, G. F.; Lieber, C. M. *Nat. Protoc.* **2006**, *1* (4), 1711−1724.
(30) Vu, X. T.; Stockmann, R.; Wolfrum, B.; Offenhäusser, A.; Ingebrandt, S. *Phys. Status Solidi A* **2010**, *207* (4), 850−857.
(31) Lebeuf, R.; Zhu, Y.; Nardello-Rataj, V.; Lallier, J. P.; Aubry, J. M. *Green Chem.* **2012**, *14* (3), 825−831.
(32) Hayashi, N.; Yoshikawa, T.; Kurakawa, M.; Ohnuma, T.; Sugiyama, Y.; Higuchi, H. *Mol. Cryst. Liq. Cryst.* **2006**, *456*, 133−137.
(33) Regeimbal, J.; Gleiter, S.; Trumpower, B. L.; Yu, C. A.; Diwakar, M.; Ballou, D. P.; Bardwell, J. C. A. *Proc. Natl. Acad. Sci. U. S. A.* **2003**, *100* (24), 13779−13784.
(34) Yadav, A. R.; Sriram, R.; Carter, J. A.; Miller, B. L. *Mater. Sci. Eng., C* **2014**, *35*, 283−290.
(35) Peled, A.; Pevzner, A.; Peretz Soroka, H.; Patolsky, F. *J. Nanobiotechnol.* **2014**, *12* (1), 7.
(36) King, J. F.; Lam, J. Y. L.; Skonieczny, S. *J. Am. Chem. Soc.* **1992**, *114* (5), 1743−1749.
(37) de Bont, D. B. A.; Sliedregt-Bol, K. M.; Hofmeyer, L. J. F.; Liskamp, R. M. J. *Bioorg. Med. Chem.* **1999**, *7* (6), 1043−1047.
(38) Zhang, A.; Sun, H.; Yan, G.; Wang, P.; Han, Y.; Wang, X. *Cancer Lett.* **2014**, *345* (1), 17−20.
(39) Fiehn, O. Metabolomics—the link between genotypes and phenotypes. In *Functional Genomics*; Springer: 2002; pp 155−171.
(40) Kaddurah-Daouk, R.; Kristal, B. S.; Weinshilboum, R. M. *Annu. Rev. Pharmacol. Toxicol.* **2008**, *48*, 653−683.
(41) Wishart, D. S.; Tzur, D.; Knox, C.; Eisner, R.; Guo, A. C.; Young, N.; Cheng, D.; Jewell, K.; Arndt, D.; Sawhney, S. *Nucleic acids research* **2007**, *35* (suppl_1), D521−D526.
(42) Nicholson, J. K. *Mol. Syst. Biol.* **2006**, *2* (1), 52.
(43) Dunn, W. B.; Broadhurst, D. I.; Atherton, H. J.; Goodacre, R.; Griffin, J. L. *Chem. Soc. Rev.* **2011**, *40* (1), 387−426.
(44) Test, S. T.; Weiss, S. J. *J. Biol. Chem.* **1984**, *259* (1), 399−405.
(45) Lacy, F.; O'Connor, D. T.; Schmid-Schonbein, G. W. *J. Hypertens.* **1998**, *16* (3), 291−303.
(46) Wurtman, R. J.; Cansev, M.; Ulus, I. H. Choline and Its Products Acetylcholine and Phosphatidylcholine. In *Handbook of Neurochemistry and Molecular Neurobiology*; Lajtha, A., Tettamanti, G., Goracci, G., Eds.; Springer US: 2010; pp 443−501.
(47) Glunde, K.; Bhujwalla, Z. M.; Ronen, S. M. *Nat. Rev. Cancer* **2011**, *11* (12), 835−848.
(48) Zhang, A. h.; Sun, H.; Qiu, S.; Wang, X. j. *Magn. Reson. Chem.* **2013**, *51* (9), 549−556.
(49) Alberti, K. G. M. M.; Zimmet, P. f. *Diabetic medicine* **1998**, *15* (7), 539−553.

DOI: 10.1021/acs.nanolett.9b00052
Nano Lett. 2019, 19, 2478−2488

(50) Som, P.; Atkins, H.; Bandoypadhyay, D.; Fowler, J.; MacGregor, R.; Matsui, K.; Oster, Z.; Sacker, D.; Shiue, C.; Turner, H. *J. Nucl. Med.* **1980**, *21* (7), 670−675.
(51) DeBerardinis, R. J.; Lum, J. J.; Hatzivassiliou, G.; Thompson, C. B. *Cell Metab.* **2008**, *7* (1), 11−20.
(52) Vander Heiden, M. G.; Cantley, L. C.; Thompson, C. B. *Science* **2009**, *324* (5930), 1029−1033.
(53) Wang, J. *Chem. Rev.* **2008**, *108* (2), 814−825.
(54) Wacharasint, P.; Nakada, T. A.; Boyd, J. H.; Russell, J. A.; Walley, K. R. *Shock* **2012**, *38* (1), 4−10.
(55) Mascini, M.; Mazzei, F. *Anal. Chim. Acta* **1987**, *192*, 9−16.
(56) Peretz-Soroka, H.; Pevzner, A.; Davidi, G.; Naddaka, V.; Tirosh, R.; Flaxer, E.; Patolsky, F. *Nano Lett.* **2013**, *13* (7), 3157−3168.
(57) Lacy, F.; O'Connor, D. T.; Schmid-Schonbein, G. W. *J. Hypertens.* **1998**, *16* (3), 291−303.
(58) Valko, M.; Leibfritz, D.; Moncol, J.; Cronin, M. T. D.; Mazur, M.; Telser, J. *Int. J. Biochem. Cell Biol.* **2007**, *39* (1), 44−84.
(59) Osborn, J. J. *Am. J. Physiol.* **1953**, *175* (3), 389−398.
(60) Coller, H. A. *Am. J. Pathol.* **2014**, *184* (1), 4−17.
(61) Warburg, O. *Science* **1956**, *123* (3191), 309−314.
(62) Kaushik, A. K.; DeBerardinis, R. J. *Biochim. Biophys. Acta, Rev. Cancer* **2018**, *1870*, 2.
(63) Stein, M.; Lin, H.; Jeyamohan, C.; Dvorzhinski, D.; Gounder, M.; Bray, K.; Eddy, S.; Goodin, S.; White, E.; DiPaola, R. S. *Prostate* **2010**, *70* (13), 1388−1394.
(64) Raez, L. E.; Papadopoulos, K.; Ricart, A. D.; Chiorean, E. G.; DiPaola, R. S.; Stein, M. N.; Lima, C. M. R.; Schlesselman, J. J.; Tolba, K.; Langmuir, V. K. *Cancer Chemother. Pharmacol.* **2013**, *71* (2), 523−530.
(65) Wiersema, M. J.; Vilmann, P.; Giovannini, M.; Chang, K.; Wiersema, L. *Gastroenterology* **1997**, *112* (4), 1087−1095.
(66) Gingras, I.; Salgado, R.; Ignatiadis, M. *Curr. Opin. Oncol.* **2015**, *27* (6), 560−567.
(67) Pelicano, H.; Carney, D.; Huang, P. *Drug Resist. Updates* **2004**, *7* (2), 97−110.
(68) Navin, N.; Kendall, J.; Troge, J.; Andrews, P.; Rodgers, L.; McIndoo, J.; Cook, K.; Stepansky, A.; Levy, D.; Esposito, D. *Nature* **2011**, *472* (7341), 90−94.
(69) Kunz-Schughart, L. A.; Freyer, J. P.; Hofstaedter, F.; Ebner, R. *J. Biomol. Screening* **2004**, *9* (4), 273−285.
(70) Patra, B.; Peng, C.-C.; Liao, W.-H.; Lee, C.-H.; Tung, Y.-C. *Sci. Rep.* **2016**, *6*, 21061.
(71) Ellis, D. I.; Dunn, W. B.; Griffin, J. L.; Allwood, J. W.; Goodacre, R. *Pharmacogenomics* **2007**, *8* (9), 1243−1266.
(72) Foo, J.; Michor, F. *J. Theor. Biol.* **2014**, *355*, 10−20.
(73) Jaeger, K.-E.; Eggert, T. *Curr. Opin. Biotechnol.* **2004**, *15* (4), 305−313.
(74) Scognamiglio, V. *Biosens. Bioelectron.* **2013**, *47*, 12−25.
(75) Shamsipur, M.; Siroueinejad, A.; Hemmateenejad, B.; Abbaspour, A.; Sharghi, H.; Alizadeh, K.; Arshadi, S. *J. Electroanal. Chem.* **2007**, *600* (2), 345−358.
(76) Esch, E. W.; Bahinski, A.; Huh, D. *Nat. Rev. Drug Discovery* **2015**, *14* (4), 248.

DOI: 10.1021/acs.nanolett.9b00052
Nano Lett. 2019, 19, 2478−2488